
VELOCITY VARIATIONS IN CROSS-HOLE SONIC LOGGING SURVEYS

Causes and Impacts in Drilled Shafts

Publication No. FHWA-CFL/TD-08-009

September 2008



U.S. Department
of Transportation
**Federal Highway
Administration**

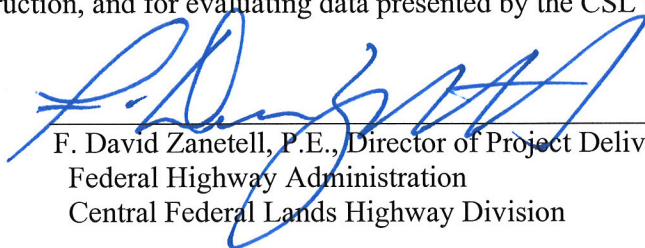


**Central Federal Lands Highway Division
12300 West Dakota Avenue
Lakewood, CO 80228**

FOREWORD

The Federal Lands Highway (FLH) of the Federal Highway Administration (FHWA) promotes development and deployment of applied research and technology applicable to solving transportation related issues on Federal Lands. The FLH provides technology delivery, innovative solutions, recommended best practices, and related information and knowledge sharing to Federal agencies, Tribal governments, and other offices within the FHWA.

This study evaluated the effectiveness of cross-hole sonic logging (CSL) for non-destructive evaluation of concrete drilled-shaft bridge foundations using numerical analysis. Effects of tube material, tube bending, concrete curing, hydration, heat transfer, residual stress, surrounding ground conditions, cracking, internal rebar support, and external loading on the seismic velocity CSL measurements are shown. This project provides designers, inspectors, and contractors with a basis for understanding basic principles of the chemistry, physics, and mechanics involved in the process of drilled shaft construction, and for evaluating data presented by the CSL technique.



F. David Zanetell, P.E., Director of Project Delivery
Federal Highway Administration
Central Federal Lands Highway Division

Notice

This document is disseminated under the sponsorship of the U.S. Department of Transportation in the interest of information exchange. The U.S. Government assumes no liability for the use of the information contained in this document. This report does not constitute a standard, specification, or regulation.

The U.S. Government does not endorse products or manufacturers. Trademarks or manufacturers' names appear in this report only because they are considered essential to the objective of the document.

Quality Assurance Statement

The FHWA provides high-quality information to serve Government, industry, and the public in a manner that promotes public understanding. Standards and policies are used to ensure and maximize the quality, objectivity, utility, and integrity of its information. FHWA periodically reviews quality issues and adjusts its programs and processes to ensure continuous quality improvement.

VELOCITY VARIATIONS IN CSL SURVEYS – TABLE OF CONTENTS

Technical Report Documentation Page

1. Report No. FHWA-CFL/TD-08-009		2. Government Accession No.		3. Recipient's Catalog No.	
4. Title and Subtitle <i>Velocity Variations in Cross-Hole Sonic Logging Surveys Causes and Impacts in Drilled Shafts</i>				5. Report Date September 2008	
				6. Performing Organization Code	
7. Author(s) Alan D. Rock, Runing Zhang, Ph.D., P.E., David Wilkinson, Ph.D.				8. Performing Organization Report No.	
9. Performing Organization Name and Address Summit Peak Technologies, LLC 6121 N. Powell Road Parker, CO 80134				10. Work Unit No. (TRAI5)	
				11. Contract or Grant No. DTFH68-05-P-00056, DTFH68-05-P-00089, and DTFH68-06-P-00105	
12. Sponsoring Agency Name and Address Federal Highway Administration Central Federal Lands Highway Division 12300 W. Dakota Avenue, Suite 210 Lakewood, CO 80228				13. Type of Report and Period Covered Final Report March 2005 – March 2007	
				14. Sponsoring Agency Code HFTS-16.4	
15. Supplementary Notes COTR: Khamis Haramy, FHWA-CFLHD. Advisory Panel Members: Michael Peabody and Roger Surdahl, FHWA-CFLHD; Matt Greer, FHWA-CO Division. and Frank Jalinoos, FHWA-TFHRC. This project was funded under the FHWA Federal Lands Highway Technology Deployment Initiatives and Partnership Program (TDIPP).					
16. Abstract <p>Drilled shafts are popular deep foundation supports, as they can be constructed in a wider range of ground conditions with less noise and vibration than driven piles. Quality assurance and quality control of drilled shafts has become a concern due to difficulties in locating defects and determining load bearing capacity. Various non-destructive evaluation (NDE) techniques have been developed to estimate the integrity of the concrete. While NDE techniques provide a powerful tool and have been widely accepted, many variables and unknowns can affect the measurement results. Results are more difficult to interpret, leading to unnecessary litigation over shaft integrity. In addition, influences of surrounding ground, stress states under different load conditions, and crack development during concrete curing further complicate determination of shaft performance.</p> <p>This study identifies various conditions that affect the load bearing capacity of drilled shafts by modeling various conditions and analyzing them with numerical methods. The analysis first identifies design criteria and construction procedures, and reviews NDE techniques. This analysis uses results based on principles and theorems from engineering mechanics, geotechnical engineering, concrete chemistry, and geophysical engineering, which are analyzed numerically by the Geostructural Analysis Package (GAP.) GAP combines numerical methods of Discrete Element Method, Particle Flow Method, Material Point Method, and Finite Differencing, together with engineering mechanics constitutive models, concrete chemistry models, thermodynamics models, and geophysical tomography and holography for geotechnical engineering application. GAP has also been used successfully for ground characterization in highway engineering and mining operations.</p> <p>This study explores many concerns recently raised for drilled shaft design, construction and maintenance. Conclusions and recommendations offer engineers more information for a better understanding of drilled shaft foundations to revolutionize foundation design, concrete mix design, construction techniques, NDE measurement, and defect evaluation, to improve performance and efficiency.</p>					
17. Key Words CROSS-HOLE SONIC LOGGING (CSL), DRILLED SHAFTS, DEEP FOUNDATION, GEOPHYSICAL SURVEY, TOMOGRAPHY, VELOCITY, ANOMALIES				18. Distribution Statement No restriction. This document is available to the public from the sponsoring agency at the website http://www.cflhd.gov .	
19. Security Classif. (of this report) Unclassified		20. Security Classif. (of this page) Unclassified		21. No. of Pages 180	22. Price

VELOCITY VARIATIONS IN CSL SURVEYS – TABLE OF CONTENTS

SI* (MODERN METRIC) CONVERSION FACTORS				
APPROXIMATE CONVERSIONS TO SI UNITS				
Symbol	When You Know	Multiply By	To Find	Symbol
LENGTH				
in	inches	25.4	Millimeters	mm
ft	feet	0.305	Meters	m
yd	yards	0.914	Meters	m
mi	miles	1.61	Kilometers	Km
AREA				
in ²	square inches	645.2	Square millimeters	mm ²
ft ²	square feet	0.093	Square meters	m ²
yd ²	square yard	0.836	Square meters	m ²
ac	acres	0.405	Hectares	ha
mi ²	square miles	2.59	Square kilometers	km ²
VOLUME				
fl oz	fluid ounces	29.57	Milliliters	mL
gal	gallons	3.785	Liters	L
ft ³	cubic feet	0.028	cubic meters	m ³
yd ³	cubic yards	0.765	cubic meters	m ³
NOTE: volumes greater than 1000 L shall be shown in m ³				
MASS				
oz	ounces	28.35	Grams	g
lb	pounds	0.454	Kilograms	kg
T	short tons (2000 lb)	0.907	megagrams (or "metric ton")	Mg (or "t")
TEMPERATURE (exact degrees)				
°F	Fahrenheit	5 (F-32)/9 or (F-32)/1.8	Celsius	°C
ILLUMINATION				
fc	foot-candles	10.76	Lux	lx
fl	foot-Lamberts	3.426	candela/m ²	cd/m ²
FORCE and PRESSURE or STRESS				
lbf	poundforce	4.45	Newtons	N
lbf/in ²	poundforce per square inch	6.89	Kilopascals	kPa
APPROXIMATE CONVERSIONS FROM SI UNITS				
Symbol	When You Know	Multiply By	To Find	Symbol
LENGTH				
mm	millimeters	0.039	Inches	in
m	meters	3.28	Feet	ft
m	meters	1.09	Yards	yd
km	kilometers	0.621	Miles	mi
AREA				
mm ²	square millimeters	0.0016	square inches	in ²
m ²	square meters	10.764	square feet	ft ²
m ²	square meters	1.195	square yards	yd ²
ha	hectares	2.47	Acres	ac
km ²	square kilometers	0.386	square miles	mi ²
VOLUME				
mL	milliliters	0.034	fluid ounces	fl oz
L	liters	0.264	Gallons	Gal
m ³	cubic meters	35.314	cubic feet	ft ³
m ³	cubic meters	1.307	cubic yards	yd ³
MASS				
g	grams	0.035	Ounces	oz
kg	kilograms	2.202	Pounds	lb
Mg (or "t")	megagrams (or "metric ton")	1.103	short tons (2000 lb)	T
TEMPERATURE (exact degrees)				
°C	Celsius	1.8C+32	Fahrenheit	°F
ILLUMINATION				
lx	lux	0.0929	foot-candles	fc
cd/m ²	candela/m ²	0.2919	foot-Lamberts	fl
FORCE and PRESSURE or STRESS				
N	newtons	0.225	Poundforce	lbf
kPa	kilopascals	0.145	poundforce per square inch	lbf/in ²

*SI is the symbol for the International System of Units. Appropriate rounding should be made to comply with Section 4 of ASTM E380. (Revised March 2003)

ABBREVIATIONS AND ACRONYMS

Acronym	Definition
ASTM	American Society for Testing and Materials
CSL	Cross-hole Sonic Logging
DEM	Distinct Element Method
DOT	Department of Transportation
FHWA	Federal Highway Administration
GAP	Geostructural Analysis Package
MPM	Material Point Method
NDE	Non Destructive Evaluation
PFC	Particle Flow Code
UPV	Ultrasonic Pulse Velocity

TABLE OF CONTENTS

CHAPTER 1. INTRODUCTION.....	1
1.1 Purpose.....	1
1.2 Cross-hole Sonic Logging (CSL) Surveys of Drilled Shafts	1
1.3 CSL Basic Theory.....	2
1.4 CSL Test Procedures and Results	5
1.5 CSL Data Processing and 3-D Tomography.....	8
1.6 Defect Definition and Drilled Shaft Integrity.....	10
CHAPTER 2. CONCRETE DEFECTS AND CURING CHEMISTRY	11
2.1 Hydration Rates and Heat Generation during Concrete Curing	12
2.2 Curing Chemistry Modeling	14
2.2.1 Empirical Modeling Methods	15
2.2.2 Geostructural Analysis Package Methods (GAP).....	15
2.3 Thermal Issues for Concrete Construction in the Field	16
2.3.1 General Aspects of Thermal Cracking Analyses.....	16
2.3.2 Problems with the 20 °C Limit.....	18
2.3.3 The Importance of Thermal Modeling in Concrete Structural Design and NDE	18
2.4 Engineering Practice for Controlling Thermal Issues in Concrete Construction	19
2.4.1 Temperature Profiling.....	19
2.4.2 Simple and Practical Techniques for Reducing Thermal Concrete Cracking With Standard Construction Techniques	19
2.4.3 Field Measures to Reduce ΔT , Techniques and Implications	21
2.5 Comparative Evaluation of Thermal Control Measures	24
2.6 Environmental Effects on Curing Chemistry and Concrete Quality	24
2.6.1 Changes in Ground Water Heat Conductivity	25
CHAPTER 3. NUMERICAL MODELING.....	27
3.1 Establishment of Numerical Model	27
3.2 Theoretical Models	28
3.3 Thermal Modeling	29
3.4 Engineering Mechanics.....	32
3.5 Discrete Element Method (DEM) Background	35
3.5.1 Discrete Element Method Definition	36
3.5.2 Equation of Motion.....	36
3.5.3 Contact Mechanics.....	39
3.5.4 Validation of Numerical Models	43
CHAPTER 4. NUMERICAL MODELING ANALYSIS OF CSL IN DRILLED SHAFTS.....	49
4.1 Geostructural Analysis Package (GAP) Model Description.....	49
4.2 Factors Affecting CSL Velocity Measurements.....	52
4.3 CSL Velocity Variations.....	55
4.4 Effect of Surrounding Material on CSL Signals.....	56

4.5	CSL Wave Interaction with Rebar	63
4.6	Tube Effects	68
4.6.1	Tube Material: PVC versus Steel Tubes	69
4.6.2	Tube Debonding.....	76
4.6.3	Sensor Drift within the Access Tubes.....	83
4.7	Concrete Cracking Effects	90
4.7.1	Concrete Strength Reduction	97
4.8	Honeycombs Effects	98
4.9	Effect of Voids	105
 CHAPTER 5. NUMERICAL MODELING OF CONCRETE CURING		111
5.1	Empirical Curing Model Method.....	111
5.2	Curing Model Presentation	113
5.3	Curing Model Simulation	114
5.3.1	Compression	114
5.3.2	Cracking.....	119
5.3.3	Heat.....	123
5.3.4	Hydration	128
5.3.5	Temperature	132
5.4	Discussion.....	135
 CHAPTER 6. NUMERICAL TESTING OF AXIAL LOAD CAPACITY OF A DRILLED SHAFT WITH ANOMALIES		137
6.1	Axial Loading Model Analysis.....	137
6.1.1	Displacement of 4 mm	139
6.1.2	Displacement of 4 cm	139
6.1.3	Displacement of 8 cm	142
6.1.4	Displacement of 12 cm	145
6.1.5	Displacement of 16 cm and 20 cm.....	147
6.2	Load-Settlement Curve Analysis	152
6.2.1	Loosened Soil.....	153
6.3	Discussion	154
 CHAPTER 7. SUMMARY, CONCLUSIONS, AND RECOMMENDATIONS FOR FUTURE STUDY.....		155
 APPENDIX A – SITE #1 VERTICAL CROSS SECTIONS		157
 REFERENCES		161

LIST OF FIGURES

Figure 1.1. Plot. Basic Wave Elements..... 3

Figure 1.2. Plot. (a) Full Waveform Stacked Traces (InfraSeis, Inc.) and (b) CSL Log Plot –First Arrival Time (FAT), Apparent Velocity and Relative Energy Versus Depth (GRL & Assoc., Inc.)..... 6

Figure 1.3. Plot. Drilled Shaft with Defects..... 7

Figure 2.1. Plot. Typical Rate of Heat Evolution during Cement Hydration 13

Figure 2.2. Plot. Temperature Plot from Data Progressively Collected from Access Tubes 20

Figure 3.1. Plot. 2D and 3D Thermal Network Mesh for Heat Conducting Calculations..... 31

Figure 3.2. Plot. Viscoelastic Contact Model for DEM..... 36

Figure 3.3. Plot. Blocks in Contact..... 38

Figure 3.4. Plot. Identical Elastic Rough Spheres in Contact..... 40

Figure 3.5. Plot. Hertz Contact of Solids of Revolution..... 41

Figure 3.6. Plot. Stack Balls Setup for Energy and Dynamic Relaxation Numerical Tests 44

Figure 3.7. Chart. Total Energy of Stack Ball 45

Figure 3.8. Chart. Dynamic Relaxation Test Results..... 46

Figure 3.9. Plot. 1-D P-Wave Propagation in a Rod..... 47

Figure 4.1. Plot. Material Palettes used in GAP Models. Defects Shown in Red Include Honeycombs, Cracking, and Debonding. Darker Colors on the Left Represent Lower Values. These Palettes are used to Display Corresponding Velocity, Wave Compression, Average Stress, Temperature, Heat Generation, Hydration Phase, Tension Strength, Modulus, etc. A Cross-section of the 1 m Drilled Shaft used in the Study is Shown on the Right. The Shaft is in the Center, Surrounded by Dry Sand, Wet Sand, Clay, and Rock. Portions of the Wet Sand, Clay, and Concrete are Hidden to Show the Internals of the Model..... 50

Figure 4.2. Plot. Location of Drilled Shaft Cross-section Surrounded by Rock 53

Figure 4.3. Plot. Location of 3D Section within Drilled Shaft 54

Figure 4.4. Plot. Rock (Top Left) vs. Clay (Top Right) at 20 μ s, with Difference (Bottom)..... 57

Figure 4.5. Plot. Rock (Top Left) vs. Clay (Top Right) at 60 μ s, with Difference (Bottom)..... 58

Figure 4.6. Plot. Rock (Top Left) vs. Clay (Top Right) at 120 μ s, with Difference (Bottom).... 59

Figure 4.7. Plot. Rock (Top Left) vs. Clay (Top Right) at 300 μ s, with Difference (Bottom).... 60

Figure 4.8. Plot. Rock (Top Left) vs. Clay (Top Right) at 500 μ s, with Difference (Bottom).... 61

Figure 4.9. Chart. CSL Signals from Rock vs. Clay, between Access Tubes 1 and 2 (Top), and Tubes 1 and 3 (Bottom) 62

Figure 4.10. Plot. No Rebar (Top Left) vs. Rebar (Top Right) at 20 μ s, with Difference (Bottom) 63

Figure 4.11. Plot. No Rebar (Top Left) vs. Rebar (Top Right) at 20 μ s, with Difference (Bottom) 64

Figure 4.12. Plot. No Rebar (Top Left) vs. Rebar (Top Right) at 120 μ s, with Difference (Bottom)..... 65

Figure 4.13. Plot. No Rebar (Top Left) vs. Rebar (Top Right) at 300 μ s, with Difference (Bottom)..... 66

Figure 4.14. Plot. No Rebar (Top Left) vs. Rebar (Top Right) at 500 μ s, with Difference (Bottom)..... 67

Figure 4.15. Chart. CSL Signals from No Rebar vs. Rebar, between Access Tubes 1 and 2 (Top), and Tubes 1 and 3 (Bottom) 68

Figure 4.16. Plot. PVC (Top Left) vs. Steel (Top Right) Access Tubes at 20 μ s, with Difference (Bottom)..... 70

Figure 4.17. Plot. PVC (Top Left) vs. Steel (Top Right) Access Tubes at 20 μ s, with Difference (Bottom)..... 71

Figure 4.18. Plot. PVC (Top Left) vs. Steel (Top Right) Access Tubes at 120 μ s, with Difference (Bottom)..... 72

Figure 4.19. Plot. PVC (Top Left) vs. Steel (Top Right) Access Tubes at 300 μ s, with Difference (Bottom)..... 73

Figure 4.20. Plot. PVC (Top Left) vs. Steel (Top Right) Access Tubes at 500 μ s, with Difference (Bottom)..... 74

Figure 4.21. Chart. CSL Signals from PVC vs. Steel Access Tubes, between Tubes 1 and 2 (Top), and Tubes 1 and 3 (Bottom) 75

Figure 4.22. Plot. Tube Debonding (Top Left) vs. No Tube Debonding (Top Right) at 20 μ s, with Difference (Bottom)..... 78

Figure 4.23. Plot. Debonding (Top Left) vs. No Tube Debonding (Top Right) at 20 μ s, with Difference (Bottom)..... 79

Figure 4.24. Plot. Debonding (Top Left) vs. No Tube Debonding (Top Right) at 120 μ s, with Difference (Bottom)..... 80

Figure 4.25. Plot. Debonding (Top Left) vs. No Tube Debonding (Top Right) at 300 μ s, with Difference (Bottom)..... 81

Figure 4.26. Plot. Debonding (Top Left) vs. No Tube Debonding (Top Right) at 500 μ s, with Difference (Bottom)..... 82

Figure 4.27. Chart. CSL Signals with Tube Debonding vs. No Tube Debonding, between Access Tubes 1 and 2 (Top), and Tubes 1 and 3 (Bottom)..... 83

Figure 4.28. Plot. Outside Sensor Drift (Top Left) vs. Inside Sensor Drift (Top Right) at 20 μ s, with Difference (Bottom)..... 84

Figure 4.29. Plot. Outside Sensor Drift (Top Left) vs. Inside Sensor Drift (Top Right) at 20 μ s, with Difference (Bottom)..... 85

Figure 4.30. Plot. Outside Sensor Drift (Top Left) vs. Inside Sensor Drift (Top Right) at 120 μ s, with Difference (Bottom)..... 86

Figure 4.31. Plot. Outside Sensor Drift (Top Left) vs. Inside Sensor Drift (Top Right) at 300 μ s, with Difference (Bottom)..... 87

Figure 4.32. Plot. Outside Sensor Drift (Top Left) vs. Inside Sensor Drift (Top Right) at 500 μ s, with Difference (Bottom)..... 88

Figure 4.33. Chart. CSL Signals with Outside Sensor Drift vs. Inside Sensor Drift, between Access Tubes 1 and 2 (Top), and Tubes 1 and 3 (Bottom)..... 89

Figure 4.34. Plot. Cracking Defect (Top Left) vs. No Defect (Top Right) at 20 μ s, with Difference (Bottom)..... 91

Figure 4.35. Plot. Cracking Defect (Top Left) vs. No Defect (Top Right) at 20 μ s, with Difference (Bottom)..... 92

Figure 4.36. Plot. Cracking Defect (Top Left) vs. No Defect (Top Right) at 120 μ s, with Difference (Bottom)..... 93

Figure 4.37. Plot. Cracking Defect (Top Left) vs. No Defect (Top Right) at 300 μ s, with Difference (Bottom)..... 94

Figure 4.38. Plot. Cracking Defect (Top Left) vs. No Defect (Top Right) at 500 μ s, with Difference (Bottom)..... 95

Figure 4.39. Chart. CSL Signals with a Cracking Defect vs. No Defect, between Access Tubes 1 and 2 (Top), and Tubes 1 and 3 (Bottom)..... 96

Figure 4.40. Plot. Honeycomb Defect (Top Left) vs. No Defect (Top Right) at 20 μ s, with Difference (Bottom)..... 99

Figure 4.41. Plot. Honeycomb Defect (Top Left) vs. No Defect (Top Right) at 20 μ s, with Difference (Bottom)..... 100

Figure 4.42. Plot. Honeycomb Defect (Top Left) vs. No Defect (Top Right) at 120 μ s, with Difference (Bottom)..... 101

Figure 4.43. Plot. Honeycomb Defect (Top Left) vs. No Defect (Top Right) at 300 μ s, with Difference (Bottom)..... 102

Figure 4.44. Plot. Honeycomb Defect (Top Left) vs. No Defect (Top Right) at 500 μ s, with Difference (Bottom)..... 103

Figure 4.45. Chart. CSL Signals with a Honeycomb Defect vs. No Defect, between Access Tubes 1 and 2 (Top), and Tubes 1 and 3 (Bottom)..... 104

Figure 4.46. Plot. Void Defect (Top Left) vs. No Defect (Top Right) at 20 μ s, with Difference (Bottom)..... 105

Figure 4.47. Plot. Void Defect (Top Left) vs. No Defect (Top Right) at 20 μ s, with Difference (Bottom)..... 106

Figure 4.48. Plot. Void Defect (Top Left) vs. No Defect (Top Right) at 120 μ s, with Difference (Bottom)..... 107

Figure 4.49. Plot. Void Defect (Top Left) vs. No Defect (Top Right) at 300 μ s, with Difference (Bottom)..... 108

Figure 4.50. Plot. Void Defect (Top Left) vs. No Defect (Top Right) at 500 μ s, with Difference (Bottom)..... 109

Figure 4.51. Chart. CSL Signals with a Void vs. No Defect, between Access Tubes 1 and 2 (Top), and Tubes 1 and 3 (Bottom) 110

Figure 5.1. Chart. Rate of Heat Generation (Cal/hr) used in the Numerical Mode..... 112

Figure 5.2. Plot. Curing Compression. Top: 4 hours. Bottom: 8 hours. Left: Rock. Middle: Clay. Right: Difference..... 116

Figure 5.3. Plot. Curing Compression. Top: 12 hours. Bottom: 24 hours. Left: Rock. Middle: Clay. Right: Difference..... 117

Figure 5.4. Plot. Curing Compression. Top: 2 days. Bottom: 3 days. Left: Rock. Middle: Clay. Right: Difference..... 118

Figure 5.5. Plot. Curing Compression. Top: 4 days. Bottom: 5 days. Left: Rock. Middle: Clay. Right: Difference..... 119

Figure 5.6. Plot. Curing Fracture. Top: 4 hours. Bottom: 8 hours. Left: Rock. Middle: Clay. Right: Difference..... 120

Figure 5.7. Plot. Curing Fracture. Top: 12 hours. Bottom: 24 hours. Left: Rock. Middle: Clay. Right: Difference..... 121

Figure 5.8. Plot. Curing Fracture. Top: 2 days. Bottom: 3 days. Left: Rock. Middle: Clay. Right: Difference..... 122

Figure 5.9. Plot. Curing Fracture. Top: 4 days. Bottom: 5 days. Left: Rock. Middle: Clay. Right: Difference..... 123

Figure 5.10. Plot. Curing Heat. Top: 4 hours. Bottom: 8 hours. Left: Rock. Middle: Clay. Right: Difference 124

Figure 5.11. Plot. Curing Heat. Top: 12 hours. Bottom: 24 hours. Left: Rock. Middle: Clay. Right: Difference 125

Figure 5.12. Plot. Curing Heat. Top: 2 days. Bottom: 3 days. Left: Rock. Middle: Clay. Right: Difference 126

Figure 5.13. Plot. Curing Heat. Top: 4 days. Bottom: 5 days. Left: Rock. Middle: Clay. Right: Difference 127

Figure 5.14. Plot. Curing Hydration. Top: 4 hours. Bottom: 8 hours. Left: Rock. Middle: Clay. Right: Difference 128

Figure 5.15. Plot. Curing Hydration. Top: 12 hours. Bottom: 24 hours. Left: Rock. Middle: Clay. Right: Difference 129

Figure 5.16. Plot. Curing Hydration. Top: 2 days. Bottom: 3 days. Left: Rock. Middle: Clay. Right: Difference 130

Figure 5.17. Plot. Curing Hydration. Top: 4 days. Bottom: 5 days. Left: Rock. Middle: Clay. Right: Difference 131

Figure 5.18. Plot. Curing Temperature. Top: 4 hours. Bottom: 8 hours. Left: Rock. Middle: Clay. Right: Difference 132

Figure 5.19. Plot. Curing Temperature. Top: 12 hours. Bottom: 24 hours. Left: Rock. Middle: Clay. Right: Difference 133

Figure 5.20. Plot. Curing Temperature. Top: 2 days. Bottom: 3 days. Left: Rock. Middle: Clay. Right: Difference 134

Figure 5.21. Plot. Curing Temperature. Top: 4 days. Bottom: 5 days. Left: Rock. Middle: Clay. Right: Difference 135

Figure 6.1. Plot. Compression Stress at Initial Vertical Displacement. Top: Sand Intrusion at 1 m Depth. Bottom: Sand Intrusion 3 m Depth. Left: Compression Stress, No Defect. Center: Compression Stress. Right: Compression Stress Difference 138

Figure 6.2. Plot. Fracture Extent at Initial Vertical Displacement. Top: Sand Intrusion at 1 m Depth. Bottom: Sand Intrusion 3 m Depth. Left: Fractures, No Defect. Center: Fractures. Right: Fracture Difference 140

Figure 6.3. Plot. Compression Stress at 4 cm Vertical Displacement. Top: Sand Intrusion at 1 m Depth. Bottom: Sand Intrusion 3 m Depth. Left: Compression Stress, No Defect. Center: Compression Stress. Right: Compression Stress Difference 141

Figure 6.4. Plot. Fracture Extent at 4 cm Vertical Displacement. Top: Sand Intrusion at 1 m Depth. Bottom: Sand Intrusion 3 m Depth. Left: Fractures, No Defect. Center: Fractures. Right: Fracture Difference 142

Figure 6.5. Plot. Compression Stress at 8 cm Vertical Displacement. Top: Sand Intrusion at 1 m Depth. Bottom: Sand Intrusion 3 m Depth. Left: Compression Stress, No Defect. Center: Compression Stress. Right: Compression Stress Difference 143

Figure 6.6. Plot. Fracture Extent at 8 cm Vertical Displacement. Top: Sand Intrusion at 1 m Depth. Bottom: Sand Intrusion 3 m Depth. Left: Fractures, No Defect. Center: Fractures. Right: Fracture Difference 144

Figure 6.7. Plot. Compression Stress at 12 cm Vertical Displacement. Top: Sand Intrusion at 1 m Depth. Bottom: Sand Intrusion 3 m Depth. Left: Compression Stress, No Defect. Center: Compression Stress. Right: Compression Stress Difference 146

Figure 6.8. Plot. Fracture Extent at 12 cm Vertical Displacement. Top: Sand Intrusion at 1 m Depth. Bottom: Sand Intrusion 3 m Depth. Left: Fractures, No Defect. Center: Fractures. Right: Fracture Difference 147

Figure 6.9. Plot. Compression Stress at 16 cm Vertical Displacement. Top: Sand Intrusion at 1 m Depth. Bottom: Sand Intrusion 3 m Depth. Left: Compression Stress, No Defect. Center: Compression Stress. Right: Compression Stress Difference 148

Figure 6.10. Plot. Fracture Extent at 16 cm Vertical Displacement. Top: Sand Intrusion at 1 m Depth. Bottom: Sand Intrusion 3 m Depth. Left: Fractures, No Defect. Center: Fractures. Right: Fracture Difference 149

Figure 6.11. Plot. Compression Stress at 20 cm Vertical Displacement. Top: Sand Intrusion at 1 m Depth. Bottom: Sand Intrusion 3 m Depth. Left: Compression Stress, No Defect. Center: Compression Stress. Right: Compression Stress Difference 150

Figure 6.12. Plot. Fracture Extent at 20 cm Vertical Displacement. Top: Sand Intrusion at 1 m Depth. Bottom: Sand Intrusion 3 m Depth. Left: Fractures, No Defect. Center: Fractures. Right: Fracture Difference 151

Figure 6.13. Chart. Effect of a Defect at Two Different Depths on Load Bearing Capacity 152

Figure 6.14. Chart. Effect of a Defect on Load Bearing Capacity with Shaft in Compacted Soil 153

Figure 6.15. Chart. Effect of Soil Compaction on Load Bearing Capacity 154

LIST OF TABLES

Table 1.1 Numerical Relationship between Path Length (PL), Transit Time (TT), Frequency (f), Period ($T=1/f$), Velocity ($V=PL/TT$), and Wavelength ($\lambda=V/f$)..... 4

Table 2.1 Properties of Typical Ceramics..... 11

Table 2.2 Compounds Involved in the Hydration Process (Kosmatka 2002)..... 13

Table 2.3 Surface Cracking Risks for a Structure with Concrete Thickness of 1.5 m 17

Table 2.4 Effects on Crack Sensitivity (Springenschmid 1998)..... 21

Table 2.5 Comparison of Measures on ΔT , Concrete Strength, and Overall Concrete Quality. 23

Table 2.6 Ground Water Flow in Soil..... 25

Table 4.1 Property Ranges Corresponding to Material Color Palettes..... 51

Table 4.2 Material Properties used in Models 51

Table 4.3 Thermal Expansion of PVC and Steel (inches/100 ft)..... 76

Table 5.1 Curing Model Coefficients 113

